Accepted Manuscript

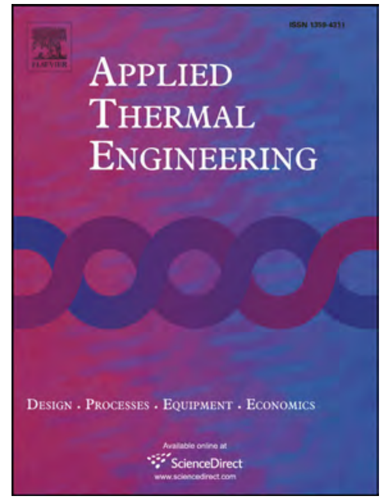

An intelligent cooling system and control model for improved engine thermal management

Arya K. Haghighat, Soheil Roumi, Navid Madani, Davoud Bahmanpour, Michael G. Olsen

PII:	S1359-4311(17)31085-2
DOI:	http://dx.doi.org/10.1016/j.applthermaleng.2017.08.102
Reference:	ATE 10985
To appear in:	*Applied Thermal Engineering*
Received Date:	18 March 2017
Revised Date:	5 August 2017
Accepted Date:	20 August 2017

Please cite this article as: A.K. Haghighat, S. Roumi, N. Madani, D. Bahmanpour, M.G. Olsen, An intelligent cooling system and control model for improved engine thermal management, *Applied Thermal Engineering* (2017), doi: http://dx.doi.org/10.1016/j.applthermaleng.2017.08.102

An intelligent cooling system and control model for improved engine thermal management

Arya K Haghighat[a, 1] Soheil Roumi [b], Navid Madani [c], Davoud Bahmanpour[d] and Michael G. Olsen[a]

[a] Department of Mechanical Engineering, Iowa State University, Ames, Iowa, USA

[b] Department of Renewable Energies and Environment, University of Tehran, Tehran, Iran

[c] IPCO, 6th Km. of Karaj Special Rd, Tehran, Iran

[d] Department of Mechanical Engineering, Amirkabir University of Technology, Tehran, Iran

HIGHLIGHTS

- An intelligent cooling system and engine cooling system model for an internal combustion engine were investigated
- The intelligent system consisted of an electrical water pump, and electrical fan, and a heated thermostat
- The model was based on engine characteristics derived from experiments on a 1.4 L engine
- The intelligent cooling system decreased fuel consumption by 1.1% and decreased hydrocarbon and CO emissions by 5.3% and 6.1% compared to a conventional cooling system under the NEDC cycle
- Engine performance was improved over all parts of the NEDC cycle, including warm up and both high and low load operating conditions

Abstract

A controlling model for the cooling system of an engine was developed in order to reduce fuel consumption and engine emissions through the use of controllable engine cooling components including an electrical water pump, an electrical fan, and a heated thermostat. The model was based on engine characteristics that were derived from experiments on a 1.4L engine. The results of simulations using the derived engine model showed that fuel consumption is decreased 1.1% and hydrocarbon and carbon monoxide emissions are reduced 5.3% and 6.1%, respectively, for the intelligent cooling system under NEDC cycle operation compared to a conventional cooling system. Engine performance was improved over all parts of the NEDC cycle, including engine warm up and both high and low engine load conditions. In non-cold start situations, the integration of an electrical water pump proved especially beneficial. For instance, if the initial coolant temperature is equal to 80°C, the energy consumption for an electrical water pump is less than half of that of a mechanical water pump. Considering both the potential fuel savings and emission reductions, it is beneficial to substitute the active controllable components described in this work for conventional mechanical components that provide insufficient cooling during various engine operation conditions while requiring greater energy to both increase fuel efficiency and reduce pollutant emissions.

Keywords

Intelligent cooling system, Thermal management, Engine efficiency, Heated thermostat, Electrical water pump, Variable speed fan

[1] Corresponding author.
E-mail address: arya.k.haghighat@gmail.com

1. Introduction

Increasing engine efficiency can result not only in fuel savings, but also in the reduction of greenhouse gases and other environmental pollutants emitted into the atmosphere. Thus, it can be both economically and environmentally beneficial to develop and improve technologies that can simultaneously reduce environmental pollutants and increase fuel efficiency in engines. Numerous studies have presented different solutions to decrease air pollutants created by road traffic[1, 2]. Among these technologies are those considering a revision of the engine cooling and the thermal needs on board the vehicle [3].

One potentially significant method for reducing air pollution is maintaining combustion conditions within an optimum temperature range related to load and engine speed. In such a case, not only will fuel consumption be reduced, but pollutant emissions will also be reduced by improving combustion operating conditions. By carefully controlling combustion temperature, pollutants resulting from incomplete combustion can be reduced or eliminated.

Thermal management of a vehicle is achieved through the combined contributions of the engine cooling system, the air conditioning system, the engine lubrication system, and the intake-exhaust system. The heat exchanger components for each of these systems are located in the engine case, where the different systems and the thermal environment interact [4].

Exhaust catalysts have had a remarkable role in decreasing pollutants, and there is a direct relation between their performance and exhaust gas temperature. Exhaust catalysts require high temperature to operate most effectively, and if they can reach their operating temperature more rapidly, then the catalysts can be more efficient in converting pollutants to harmless gases. Thus, controlling engine temperature, and hence, catalyst temperature, can lead to a reduction in pollutant emissions [5, 6].

Numerous engine cooling strategies, including nucleate boiling, Thermal Management Intelligent System (THEMIS), and Cool Master have been developed in the past, and these systems have improved conventional cooling system performance by either replacing conventional cooling components or adding electrical components. Implementation of such alternative strategies for engine cooling has been shown to improve engine efficiency and performance [7].

In the nucleate boiling strategy, cooling is achieved through the thermal latent heat of evaporating water. In this method, accumulation of steam should be avoided, as this can reduce the convective heat transfer coefficient. To prevent steam accumulation, an expansion tank is used which results in a 5°C to 10°C rise in cylinder head temperature. Fuel consumption has been found to decrease about 2-3 percent in a MVEG (Motor Vehicle Emissions Group) cycle [8].

In the THEMIS strategy, by using an electrical valve, an electrical water pump, and a variable speed fan instead of a conventional thermostat, water pump, and fan, the cooling system can be controlled efficiently and continuously. Implementation of this strategy can result in a cylinder temperature rise of 30°C and a corresponding fuel consumption reduction of around 5 percent [9, 10]. However, changes in pollutant emissions must also be considered.

The Cool Master strategy is similar to THEMIS, except that a mechanical water pump is used to circulate water, and a small electrical pump is used to control the cabin environment. The other components are similar to those used in THEMIS, and the resulting cylinder head temperature and fuel consumption improvement are similar to those reported for THEMIS [11, 12].

One analysis method for evaluating cooling strategies focuses on the integration of cooling models into the framework of a vehicle dynamics simulation including transient engine performance demonstrated on a modern passenger car. In this approach, analyses are performed for two drive cycles featuring considerably different velocity profiles to reveal their impacts on the operational principles of the powertrain components and their interaction. The results of this type of analysis indicate for both drive cycles fuel reduction due to the integration of an electric water pump is relatively small, with fuel savings of between 0.75% and 1.1% [13].

One of the most crucial periods of the driving cycle is warm-up[14]. During warm-up, fuel consumption and pollutant production rise[15]. Thus, reducing warm-up time can both increase engine efficiency and decrease emissions[16]. One technique to lessen heat loss during warm is to use oil to cool exhaust gas recirculation (EGR) gases along with a number of coolant flow control valves. A 2.4L diesel engine equipped for this technique was run over a cold start NEDC (New European Driving Cycle) with four flow strategies as a screening exercise to characterize the behavior of such a system. As can be seen in Table 1, the throttle coolant, EGR coolant, and oil pump flow control are the key components of the various strategies considered[17].

Condition	Engine out coolant throttle	EGR cooler coolant flow	EGR cooler	VFOP
Uncontrolled	NC[1]	NC	Coolant	Max
Baseline	NC[1]	NC	Coolant	C[1,4]
Build 2	Mapped[2]	NC	Oil	C[1,4]
Build 3	Mapped[3]	Restricted	Oil	C[1,4]

[1] C=Controlled, NC= Non Controlled

[2] Build 2 mapped coolant flow inhibits coolant flow until a head metal temperature of 95°C is reached and then opens as a function of head temperature and engine speed

[3] Similar to Build 2, only throttle opening occurs at 105°C engine head temperature

[4] Control oil flow is based on target oil gallery pressure of 2 bar

NOTE: Oil cooler coolant flow is opened in all conditions.

Table 1. Experimental setup for detailed analysis[17]

The main difference between the strategies labeled Build 2 & 3 is the throttle opening temperature which occurs at 95 and 105°, respectively. Fuel consumption in the Build 2 strategy showed reductions of up to 4 per cent, but this benefit was offset by a 3 per cent increase in nitrogen oxide (NOx) emissions [17, 18]. NOx emissions could be reduced by throttling the flow, so that the mass of coolant in the degas bottle and radiator could be isolated from the system during warm-up, essentially reducing the thermal inertia. Heat transfer directly to the oil from the EGR gases rather than from the coolant permitted more heat to be transferred into the oil, resulting in engine oil supply temperature increases of up to 6°C. While this strategy corresponds to the quicker warm-up and to delays in injection timing and reduces NO_x emissions, it also compromised overall fuel consumption benefits [19, 20]. Finally, the analysis revealed that the engine-out coolant, the EGR coolant loop, and the oil cooler coolant flow must be controlled to optimize such a thermal management system [21, 22].

In an alternate approach, researchers have attempted to improve engine performance by adding electronic components to the cooling system [23, 24]. This is the approach in the work considered here. For example, one component that has been applied to reduce energy consumption and emission production is an enhanced electric water pump [25]. Compared to conventional water pumps, electric clutch water pumps have been demonstrated to improve engine function [26]. Another example is a variable position thermostat (VPEMT). A significant reduction in the duration of the warm-up period can be achieved using VPEMT control. Results indicate that by using a Modification coolant system (MCS) with VPEMT control, the engine temperature increases more rapidly, and a reduction in the engine warm-up period of approximately 28.5% can be achieved [27]. The MCS enables reduction of the coolant flow rate by more than 23.5% during the cold start (transient) phase and 15.2% at steady state (i.e., fully warmed-up) compared to the original system flow rate under NEDC operation [28].

A comparison of the previously described techniques for increasing cooling system behavior shows the use of electronic components combined with nonlinear control methods to be the most promising [29, 30]. For this reason, the engine cooling strategy that is investigated in the work presented here is based on an electronic control unit (ECU) regulating engine temperature. Specifically, this work analyzes the effects of adding three new controller components within an electronic component strategy based on optimal operation conditions (this strategy is referred to in this paper as the *engine protection model*), and the resulting fuel savings and emission reductions are determined for NECD operation. The comparison is made by developing engine cooling models for both a conventional engine cooling system and also an electronic cooling system controlled by the ECU and using the model to compare engine performance. These comparisons were performed for the EF4 engine. The technical information for this engine is presented in Table 2.

Engine	EF4
Displacement	1397 cc
Fuel System	Dual (CNG and Gasoline)
Stroke	4-stroke
Max. Power	70 KW on gasoline and 62 KW on CNG mode at 6000 rpm
Max. Torque	125 N.m on gasoline and 111 N.m on CNG mode at 3250 rpm

Compression Ratio	11:1
Valves	16-valve, DOHC, CVVT

Table 2. Characteristics of the engine under investigation

2. Components of the intelligent cooling system

Three electronic cooling system components are used in the investigated intelligent cooling system. These components are an electrical fan, an electrical thermostat, and an electrical water pump. Each of these devices is described in the following section.

2.1. Electrical fan

For many years, engine fans operated such that when hot water entered the radiator, the fan simply rotated at maximum speed to cool the hot radiator water without consideration of the rate of cooling demand [31]. With improvements in electrical system control, it was possible to control the fan speed either at multiple fixed speeds or to operate it with continually variable speed. Many modern vehicles, including the BMW E46 and the TOYOTA Adventure 2001 use continually variable speed fans [32]. In this investigation, a variable speed fan with three incremental fixed speeds (off, low speed or 1000 RPM, full speed or 2000 RPM) was considered.

2.2. Thermostat

In conventional cooling systems, a wax thermostat placed at the entrance to the radiator is used to open or close the coolant route through the radiator. When water temperature rises, the wax melts and expands, forcing the thermostat valve open. The wax usually begins to melt at around 80°C and as a result, the valve may open too soon, resulting in unwanted early cooling. Two thermostat modifications can be introduced to improve the control strategy [33]. These modifications are the introduction of an electrical valve or the introduction of a heated thermostat.

In using an electrical valve instead of using a conventional wax thermostat for regulating flow through the radiator, a thermal sensor is used to continuously measure the water temperature. An electrical control unit (ECU) receives these temperature data and then regulates the voltage of a servo-motor electrical valve. The electrical valve throttles the flow of water through the radiator.

A heated thermostat is similar to a conventional wax thermostat, but it also contains an electrical heater inside the wax. In the heated thermostat, the wax begins to melt at 120°C instead of 80°C as in the conventional thermostat, and the melting of the wax is controlled by activating the electrical heating element.

The use of an electrical valve has several advantages compared to using a heated thermostat. These advantages include less thermal shock, a faster response time, better flow control, less engine fuel consumption, and lower engine emissions. However, in a malfunction situation where the electrical circuit controlling the valve does not operate properly, water temperature can rise and the engine could face catastrophic damage. In this regard, a heated thermostat is advantageous, because if a problem arises with the electronic control of a heated thermostat, the wax will still be melted by hot water (albeit, at a higher temperature than for a conventional wax thermostat) and the coolant will still flow through the radiator, preventing damage to engine. For these reasons (as well as its lower cost) a heated thermostat was chosen for use in this investigation.

2.3. Electrical water pump

In a conventional water pump, the pump shaft is directly connected to crankshaft, thus the pump's rotational speed depends entirely on the engine rotational speed and is not related to cooling demand [34]. Alternately, water pump rotational speed can be regulated according to cooling demand, and the pump can be driven with an electrical motor [35]. An ECU can be programmed to determine the necessary coolant flow rate, and the water pump speed can be adjusted by supplying the corresponding voltage to the electric motor [36]. In the present work, such an electrical water pump was used.

3. Control strategy

The energy released from fuel combustion in the engine can be divided into three parts. Some of the energy is converted into work. Another portion heats the combustion products that exit the engine through the exhaust pipe and are responsible for the warming of the engine. The final part dissipates through the surface of the engine and the cooling system to atmosphere[37]. Modern engines are capable of transforming approximately 50 percent of total energy released in combustion into work.

Because high temperatures can damage engine parts, excess heat must be ejected by the cooling system [38]. The temperatures of all crucial locations in the engine should be controlled to protect them from damage. By considering heat transfer relations between various engine locations and measuring temperature at only a few engine locations, it is possible to measure and control temperature throughout the entire engine. The heat transfer relations between different engine locations can be found in Wagner et al. [39]. In order to determine the optimal temperature of the coolant and the cooling system capabilities, the engine rotation speed, the engine load, the ambient temperature, the coolant temperature, and the vehicle's speed should be known.

3.1. Determining optimal temperature

One of the important factors in determining the optimal coolant temperature is friction. Oil viscosity varies with temperature, so as the oil temperature changes, engine friction will also change. Research has shown that at half load, friction may decrease by up to 10 percent due to the increase in lining temperature (although in this situation dry friction may possibly increase) [9]. The minimum friction usually occurs in the middle course of a piston stroke, since near that location the piston moves at maximum velocity. Maximum friction occurs at the two ends of the piston stroke where the speed of the piston is much lower. One factor preventing high temperatures in the lining is oil viscosity reduction, which results in mixed-friction at piston dead centers. Although a 30°C rise in temperature will increase friction at the piston dead center, the total friction loss over the entire range of piston motion will actually decrease by 20 percent due to the decrease in oil viscosity corresponding to this temperature rise [9].

When the engine is working in a partial load situation, increasing engine temperature can result in more efficient combustion. For example, increasing engine temperature to approximately 110°C will decrease fuel consumption by up to 5% and decrease emissions by up to 20% for CO and 10% for HC [5]. On the other hand, when the engine is operating in a full load situation (such as when climbing a hill), the resulting high temperatures can cause harmful engine knocking. Thus, temperature should be decreased in full load situations.

A series of measurements was designed to determine the optimum temperature for a given engine loading. In order to find this optimum temperature, the radiator was submerged in a pool of water kept at constant temperature. The setup for the submerged radiator is shown in Fig. 1. Then for different engine loadings (where the loadings were measured using a dynamometer) and different engine temperatures (fixed by the constant temperature bath), the fuel consumption for each case was measured. In these measurements, the fuel consumption of the engine under a given loading was determined for engine temperatures ranging between 110 C and 70 C. From these data, it was possible to find the optimum temperature, i.e., the temperature at which the engine consumes the least amount of fuel. The experimental setup for these measurements is shown in Fig. 2. The results are plotted in Fig. 3 and show that the optimum temperature is inversely proportional to the loading of the engine.

Figure 1: A photograph of the **r**adiator submerged in a constant temperature pool in order to keep the radiator temperature constant

Figure 2a. A photograph of the experimental setup for measuring optimum engine temperature

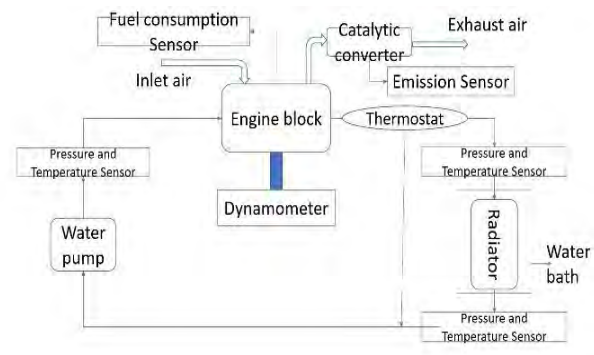

Figure 3b. A sketch of the experimental setup for measuring optimum engine temperature

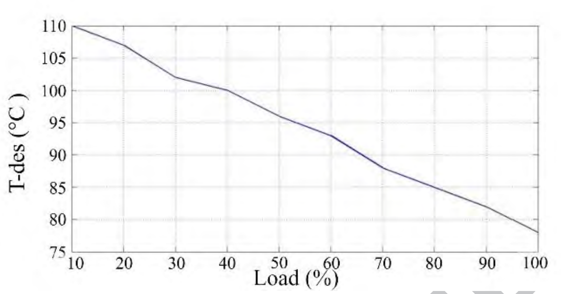

Figure 4. Optimum engine temperature as a function of engine loading

3.2. Control model

There are two types of heat that must be removed by the radiator, static heat and hysteresis heat. Static heat is the heat transferred to the cooling system at a fixed engine rotational speed and load in order to keep the engine temperature at a specific value. Hysteresis heat is the coolant heat that must be removed so that the engine temperature will decrease by a fixed amount, for example, from 110°C to 90°C.

After determining the hysteresis heat, static heat, and the engine block temperature, the engine protection model can be developed. In making these calculations and developing the model, the step delay time should be considered. Step delay is the lag of the system in response to new operating conditions.

The amount of heat that the radiator can remove can be calculated using the ambient temperature, the vehicle speed, and the coolant temperature. Then, by considering any heat needed for cabin comfort, the heater coolant flow can be determined. By using this model, it is possible to specify the radiator coolant flow (and hence, the required thermostat opening to provide that flow) and the amount of heat that must be removed by the radiator (and thus, the required fan speed and water pump rotational speed) [8].

All measurements and calculations have been performed with respect to the NEDC cycle, which is a combination of city and highway driving. By determining the proper input parameters, the engine protection model can be designed.

To determine static heat, a test procedure was designed. Heat generation was measured for different engine loads and engine rotational speeds while keeping radiator temperature constant. In this way, the necessary heat rejection in order to keep the water pool's temperature constant was measured. These measurements were then compiled into diagrams which could be used for predicting the static heat. The results of these measurements are used as inputs for engine protection model. One example of such a diagram is shown in Fig. 4. These measurements show that with increasing coolant output temperature, static heat decreases. They also show the expected result that static heat increases with increased engine load. For the NEDC cycle, it was found that the maximum static heat in city driving is 18 kW, while the maximum heat generated on the highway increased to 24 kW.

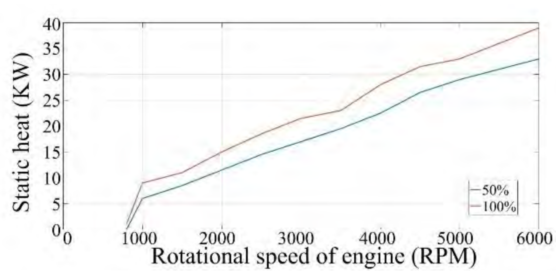

Figure 5. Static heat generation based on the load and RPM

To avoid engine knocking in full load situations, the engine should operate at lower temperature. Accordingly, another test procedure was designed to determine what engine temperature can eliminate knocking and also to determine the necessary amount of heat that must be removed to ensure that the engine block reaches this desired temperature. This test was performed for different engine speeds with the engine temperature initially fixed at 110°C, and then by changing the pool's water suddenly, this temperature was decreased to 90°C. During this cooling, the amount of heat removed by the radiator was measured. The results from one of these measurements are shown in Fig. 5. By integrating the area under the heat-time curve, the hysteresis heat due to cooling the engine from 110°C to 90°C was determined.

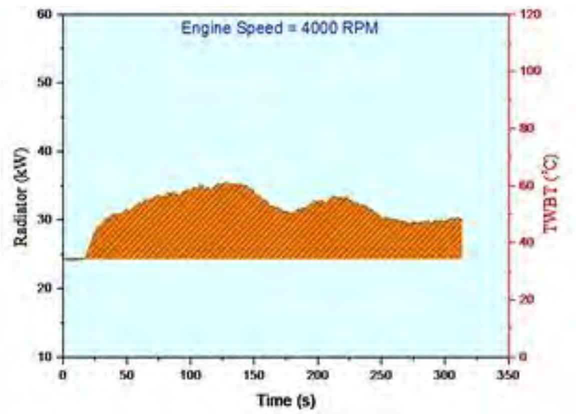

Figure 6. Estimating hysteresis heat by studying repelled energy through radiator

In developing the engine protection model, it is necessary to determine coolant and air flow rate for the engine. Vehicle speed and fan speed are the contributing factors to air speed through the radiator. Hot wire anemometry measurements have been performed to measure air speed through the radiator. In these experiments three 1 HZ sensors were placed at the radiator locations shown in Fig. 6, and air speed through the radiator was measured for various vehicle speeds for the three set fan speeds (off, low speed or 1000 RPM, full speed or 2000 RPM). In these experiments, the air speed contribution of the moving vehicle was simulated by performing measurements for a fixed engine in a wind tunnel. The results of these measurements are shown in Fig. 7.

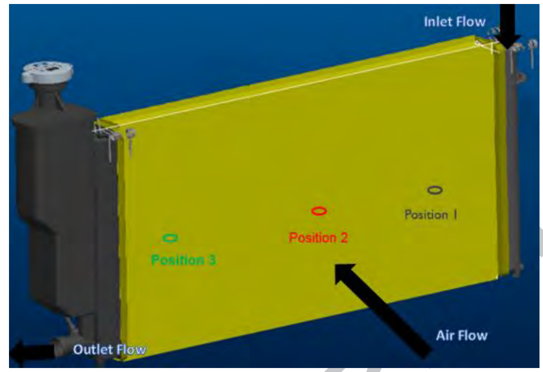

Figure 7. Schematic of radiator and attached sensors for measuring the air flow

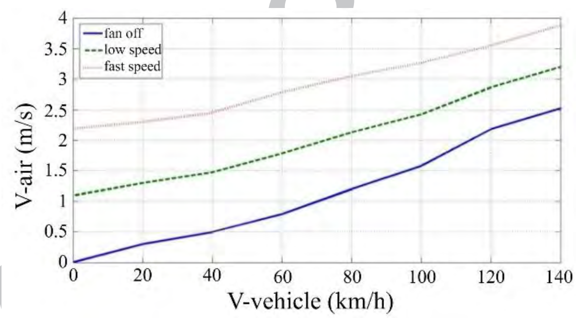

Figure 8. Mean Air flow through radiator for various fan and vehicle speeds

The thermostat opening level and the water pump speed are the contributing factors on water flow through the radiator. Using data for these factors, it is possible to obtain equation (1) for coolant flow through radiator.

$$Q_{rad} = \alpha \times F(RPM) \tag{1}$$

By using measurements from the radiator experiments and fitting a curve by least square criteria with MATLAB, the parameter α can be determined. From these data, equation (2) was derived.

$$\alpha = 2.06\sqrt{\frac{X}{X_{\max}}} \tag{2}$$

where X is the instantaneous thermostat opening, and X_{max} is the maximum thermostat opening level of 8 mm.

Equation (3) can be used to determine the function, F, with data obtained from the radiator experiments such that

$$F(RPM) = RPM \times \frac{Q_{RPM,Max}}{RPM_{\max}}$$
(3)

where $Q_{RPM,\ Max}$ is coolant flow when the engine is operating at RPM_{max} = 6000 rpm, and the thermostat is fully opened.

Finally, the amount of heat that is removed by the radiator can be determined using the water pump rotational speed and vehicle speed. To determine the amount of heat rejected in the radiator, an EF4 (A 1.4L engine which is designed by IPCO) engine was put under a "cooling functional test" in the laboratory. In this experiment, the car speed varied between 0.2-10 m/s (0.72-36 km/hr), while the amount coolant entering the radiator varied between 0-160 L/min, with the varied flow rates generated by the water pump. Since Q_{rad} is only dependent on temperature difference in a closed loop, by placing temperature sensors at the two radiator ends, Q_{rad} was calculated. Figure 8 shows the removed heat as a function of coolant flow through radiator for the case where the temperature difference between the initial air temperature and coolant temperature is 75°C. From these data, the removed heat can be determined for other temperature differences proportionally.

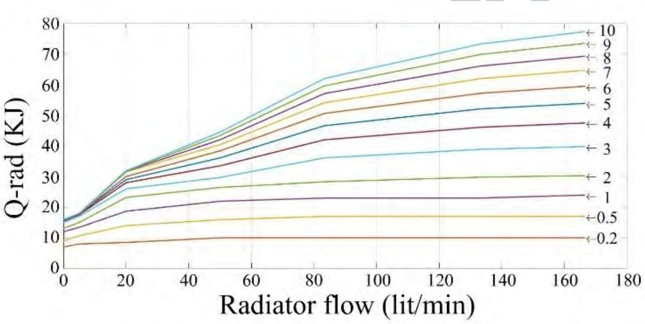

Figure 9. Repelled heat for various coolant flow rates through the radiator with an initial temperature difference of 75°C

In modeling the electronic control unit and comparing its performance to a conventional cooling system, it is necessary to explain the effects of temperature on the opening of a conventional thermostat. Assuming the relationship between temperature and thermostat opening is linear, the thermostat opening can be described by equation (4) [10]:

$$x = \begin{cases} 0 & ;if \quad (T_{cool} < T_{\min}) \\ (T_{cool} - T_{\min})/(T_{\max} - T_{\min}) & ;if \quad (T_{\min} < T_{cool} < T_{\max}) \\ 1 & ;if \quad (T_{cool} > T_{\max}) \end{cases}$$
(4)

where x is the percentage that the thermostat is open compared to being fully open.

In this equation:

$$T_{\min} = T_{sp}(1-c)$$
(5)

$$T_{\max} = T_{sp}(1+c)$$
(6)

where T_{sp} is a specified temperature midway between the temperature at which the thermostat begins to open and the temperature at which the thermostat is fully open, and c is a constant tolerance defined by the difference between the specified temperature and the initial opening and fully open temperatures [10]. For example, if a thermostat begins to open at 80°C and it would be fully opened at 92°C, then T_{sp} would be 86°C and c would be equal to 6°C. In a conventional thermostat system, for an increasing temperature process, the initial thermostat opening temperature occurs at 88°C, and thermostat becomes fully opened at 94°C. When the temperature falls, the initial closing temperature is 92°C, and at 86°C, the radiator path is completely closed.

One important characteristic of equation (4) is that it does not include any time dependence in modeling the opening or closing. In other words, it models the thermostat behavior as operating at the steady state for any given temperature. However, in a truly dynamic model the speed of the opening and closing of the thermostat must be considered.

Heated thermostats work differently than conventional thermostats. In a heated thermostat, the opening and closing is controlled by regulating voltage to a heating element. The dependence of temperature on heated thermostat opening as described by the manufacturer is shown in Fig. 9.

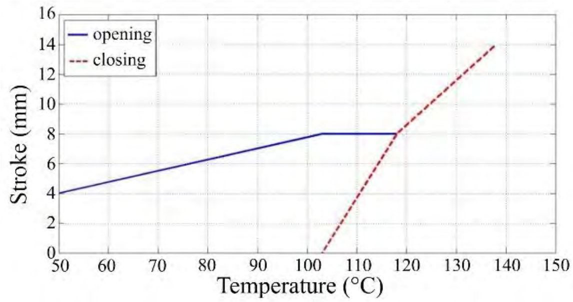

Figure 10. Heated thermostat opening level for different temperatures for both thermostat opening and closing

To accurately control the cooling system, it is necessary to consider the speed of thermostat opening and closing. This can be determined experimentally. To measure this, a closed thermostat was submerged into a water bath at a temperature of 125°C. In this situation, the thermostat was found to open at a rate of 0.5 mm per second. A similar experiment was performed on a fully opened thermostat to measure closing speed by submerging it in a water bath at a temperature of 70°C. The results show that the closing process is slower than the opening process with a closing rate of 0.4 mm per second.

Next, the coolant flow produced by the water pump must be estimated. The temperature difference between the inlet and outlet coolant is set at 5°C to avoid temperature shock in the engine block. Also, the minimum water pump rotational speed is 1000 rpm. After passing through the radiator, the radiator coolant is combined with bypass flow. To estimate the temperature of the coolant entering the engine, it is necessary to measure the flow and temperature of the bypass coolant as well as radiator coolant flow and temperature. This was done in the test engine using thermocouples at the inlet and outlet of the bypass to measure the coolant temperature and measuring the coolant flow rate through the radiator. Using these experimental measurements, the flow rate of bypass coolant can be calculated using equation (7):

$$Q_{Bypass} = (1 - \frac{X}{X_{\max}})^{\frac{1}{2.06}} \times RPM \times \frac{Q_{RPM_{\max}}}{RPM_{\max}} \quad (7)$$

T_{mix}, the temperature of the combined radiator and bypass flow can be calculated using equation (8) if constant specific heat for the coolant is assumed

$$T_{mix} = \frac{(T_{rad} \times \dot{m}_{rad} + T_{Bypass} \times \dot{m}_{Bypass})}{\dot{m}_{rad} + \times \dot{m}_{Bypass}} \quad (8)$$

Finally, to complete the engine cooling cycle, it is necessary that after the coolant is cooled in the radiator, it is returned to engine and heated again. Because the mass of coolant must be conserved, the volume of coolant (Δv) entering the engine must be the same as the volume leaving the engine.

The time interval between the coolant entering and leaving the engine depends on both the engine coolant capacity and the coolant flow rate. To calculate the coolant exit temperature at the next time step in the numerical model, it is assumed that coolant with volume (Δv) and temperature of $T_{out-previous\ step}$, will be replaced with the same volume of coolant at temperature T_{mix}. It is assumed that in this step the volume of coolant entering the tank is $v_{eng} - \Delta v$, and its temperature is equal to the coolant temperature that left the engine at the previous step. The temperature of the fluid exiting the engine in the next time step, $T_{out\_next\_step}$, can be calculated using equation (9):

$$T_{out\_next\_step} = \frac{T_{mix} \times \Delta v + T_{previous\_step} \times (v_{eng} - \Delta v)}{v_{eng}} \quad (9)$$

This coolant is now ready to remove heat from the engine, and its temperature will increase by receiving hysteresis and static heat.

The intelligent cooling system model is then formed by integrating all of the previously described individual model components into a single model. This model is shown schematically in Fig. 10.

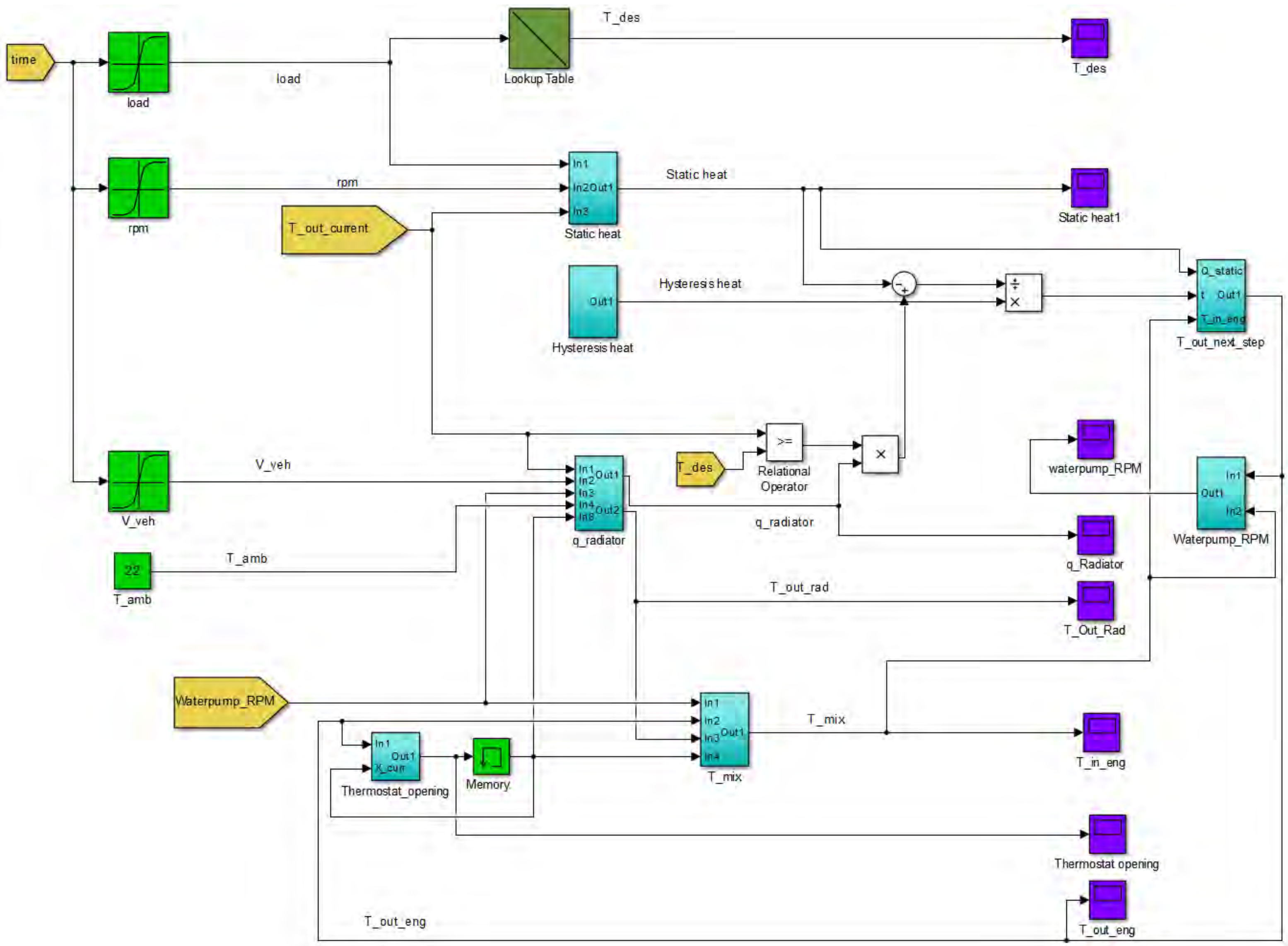

Figure 11. Intelligent cooling system strategy

4. Validation

Using the results from the experiments for a conventional cooling system consisting of a conventional thermostat, a fixed speed water pump, and a fan that simply toggles between on and off, it is possible to perform a validation of the model used in the simulation. In performing this validation some modifications must be made to the model, such as equating the rotation speed of the water pump and rotation speed of the engine, and modifying Eqn. 4 by removing the heating element so it simulates the opening of a conventional thermostat. The other modification is adjusting the fan speed so that it operates between only two speeds, on at 2000 RPM or off. The results of the simulation and experiment for coolant temperature in this conventional system are compared in Fig. 11.

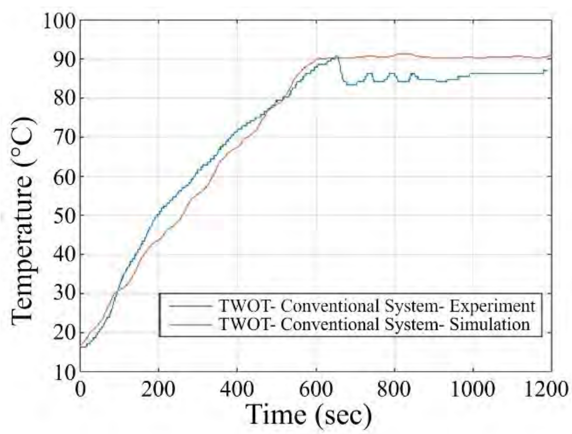

Figure 12. Simulated coolant temperature versus experiment temperature for a conventional engine cooling system

In this comparison, the simulated temperature accurately mimics the measured temperature during engine warm up. Upon the simulation reaching the engine steady state temperature, the experimentally measured temperature drops below the simulation temperature with an initial deviation of 7 °C. This deviation decreases as time increases, and 1000 seconds into the simulation (corresponding to 350 seconds after the experimentally observed decrease in temperature) the deviation between simulation and experiment is only 4 °C. As can be seen in Fig. 11, upon the initial opening of the thermostat, coolant that had been in the radiator at ambient temperature enters the cooling loop and decreases the engine coolant temperature suddenly. The difference between the experiment and simulation comes from this sudden fall in temperature.

5. Simulation results

The model was then used to compare the performance of the conventional cooling system with the intelligent cooling system. Figure 12 shows a comparison between desired coolant exit temperature, conventional cooling system temperature, and intelligent cooling system temperature during the NEDC cycle. The desired temperature is obtained from the previously described experiments that determined the temperature which results in optimum fuel efficiency for a given engine load. As expected, one effect of the intelligent cooling system is to increase mean steady state temperature by 14°C compared to the conventional cooling system. Note that for safety purposes (i.e., to prevent engine damage from knocking) the mean desired temperature is set at 104°C instead of 110°C. This is because the instantaneous temperature can rise up to 6°C above the mean temperature, thus setting the mean temperature at 104°C keeps the instantaneous temperature peaks below the 110°C threshold for knocking.

Another effect of the intelligent cooling system is that the coolant temperature leaving the engine and the desired coolant exit temperature are nearly the same, and this similarity reduces fuel consumption compared to the conventional cooling system by approximately 1.1%. Also, the intelligent cooling system is able to achieve this fuel savings while simultaneously decreasing HC and CO emissions by approximately 5.3% and 6.1 % compared to the conventional system. Note that, in this scenario we assumed that the electrical water pump has the same efficiency of the mechanical water pump; however, there are usually inefficiencies in conversion of energy which result in a smaller gain in fuel efficiency than the one predicted above.

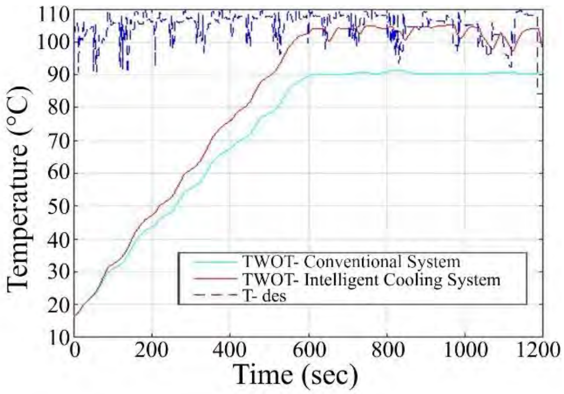

Figure 13. Desired temperature, conventional engine outlet coolant and ICS engine outlet coolant in the NECD cycle

In both the conventional and intelligent cooling systems, the thermostat is initially closed, and no coolant enters the radiator until the temperature reaches either the set point for the heated thermostat or the wax melting point in the conventional thermostat. Because of the lack of coolant flow into the radiator, the radiator temperature will be equal to ambient air temperature during this time. As the thermostat opens for the first time, the cold coolant from inside the radiator flows into the engine, and engine temperature suddenly decreases. This rapid temperature decrease not only results in deviation from the desired temperature, but also results in thermal shock in the engine block. This thermal shock also occurs in subsequent thermostat openings; however, because of coolant mixes due to previous thermostat openings, the mean coolant temperature is higher, so the resulting thermal shocks are less severe.

The opening history of the heated thermostat for the intelligent cooling system during the NEDC cycle is shown in Fig. 13. The thermostat is closed for the initial 700 seconds of the cycle, and during this time the coolant temperature increases to 104°C. After the warm-up portion of the cycle and during road driving the thermostat is often open, because during this portion of the driving cycle, the engine load is higher and additional heat must be discharged through radiator.

In the intelligent cooling system, the water pump operates at the minimum speed of 1000 rpm when the engine starts up, and this speed can increase to higher rpm if there is a greater engine cooling need. This intelligent operation reduces the energy consumption of the water pump by up to 50 % compared to a constant speed water pump for the NEDC cycle.

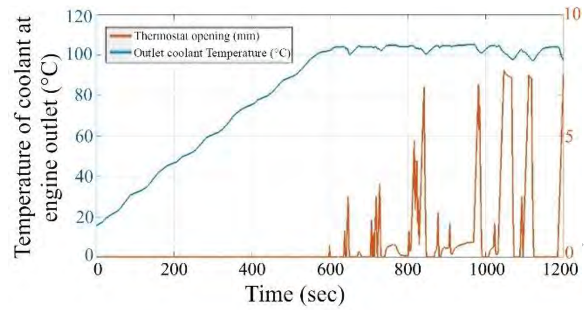

Figure 14. Heated thermostat opening or the intelligent cooling system in NEDC cycle

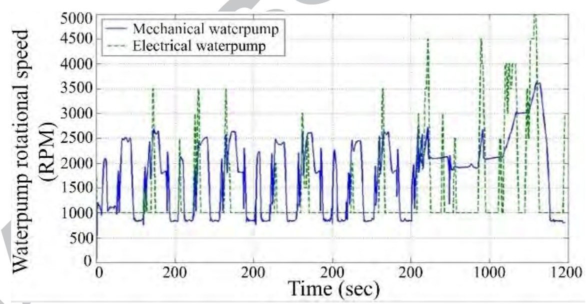

Figure 15. Comparison of water pump rotational speed for both the conventional (mechanical water pump) and intelligent (electrical water pump) cooling systems in NEDC cycle (initial temperature of coolant = 80°C)

Figure 14 compares the rotational speed for a mechanical water pump (used in the conventional cooling system) with an electrical water pump (used in the intelligent cooling system) during the NEDC cycle. As this figure shows, except for some short duration "spikes" during which the electrical water pump operates at a higher speed than the mechanical one, most of the time the electrical pump operates at a lower speed and consumes less energy. Indeed, over the 1200 seconds of the NEDC cycle, the mean rotational speed of the electrical pump was only 1316 rpm compared to 1772 rpm for the mechanical pump. This difference is also apparent when one considers only highway driving. For the highway driving portion of the NEDC, the mean rotational speed of the electrical pump was only 1811 rpm compared to 2169 rpm for the mechanical pump. While this difference, may not seem very significant, for long road trips the resulting energy conservation would be considerable.

According to spread curve of the NEDC cycle, as shown in Fig. 15, the engine primarily operates at less than 45% of full load, operating in this condition 90% of the time during the NEDC cycle. Recall that at moderate loads, an increase in engine temperature corresponds to a decrease in fuel consumption based on the experimental results on optimum engine temperature previously described in section 3.1. As a result, increasing engine temperature to 104°C using the intelligent cooling system results in more efficient operation at moderate loads compared to a conventional cooling system.

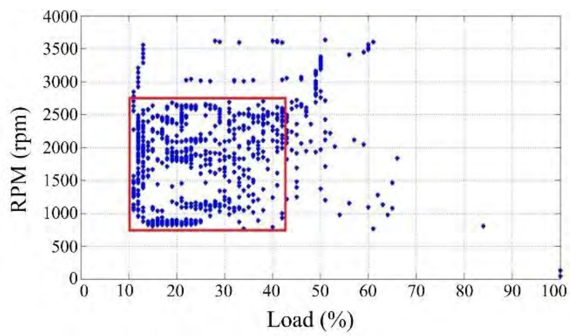

Figure 16. Spread curve of engine speed (RPM) vs. load throughout the duration of the NEDC cycle

Recall that to help avoid engine knocking, at full load conditions the engine temperature should be lowered. By measuring the hysteresis heat for different rotational speeds of the engine, it was found that hysteresis heat is independent of the engine rotational speed. As a result, the amount of heat that must be removed to decrease the coolant temperature from 110°C to 90°C is same at all engine rotational speeds.

According to the simulation results, the intelligent control system increases the engine temperature at low loads resulting in a decrease in fuel consumption. However, at high loads, in order to prevent engine knock in the cylinder, a reduction in engine temperature is desirable. Fuel consumption based on the experimental results at 70°C and 90°C is compared in Fig. 16. This figure shows the difference in fuel consumption for coolant temperature in the outlet of the engine equal to 70°C compared to fuel consumption for 90°C outlet temperature. Figure 16 compares this parameter in terms of ENSP (Engine Speed) and BMEP (Brake Mean Effective Pressure). As can be seen in Fig. 16, decreasing engine outlet coolant temperature for low load situations that are safely below the knocking temperature results in additional heat losses that lead to an increase in specific fuel consumption (corresponding to the region in Fig. 16 with mean effective pressure between 2 bars and 6 bars). As previously described in Section 3.1 for determining the optimum operation temperature, this diagram can be used to determine the temperature at which an engine will consume the minimum amount of fuel for a given load.

In high load situations where engine knocking could potentially be a concern due to high temperatures, decreasing the engine outlet coolant temperature reduces the possibility of engine knocking while also decreasing fuel consumption. However, if engine temperature is decreased too much, the effect of increasing heat loss becomes more significant than the reduction in knock possibility, and the specific fuel consumption will increase. Thus, simultaneously increasing fuel efficiency while eliminating knocking requires a careful control of engine temperature.

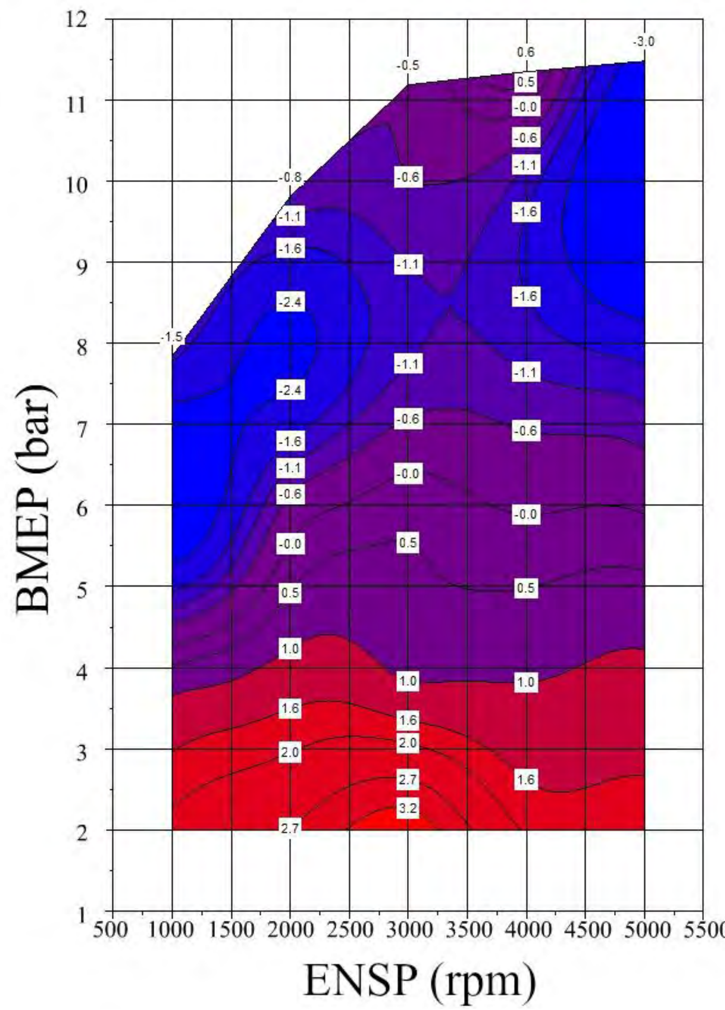

Figure 17. Consumption proportion between 70 °C and 90 °C

It has been shown that the cooling system performance can be improved by the individual contributions of both an electric water pump and a heated thermostat. However, it should also be considered that sometimes both of these devices may activate simultaneously. In situations such as this, the best solution should be selected, i.e., whether it is better to have either device operating, or one device individually. Figure 17 compares mechanical water pump speed (which is independent of outlet temperature difference because it is coupled to engine speed) and electrical water pump rotational speed for various engine inlet and outlet temperature differences ranging from 5°C up to 8°C.

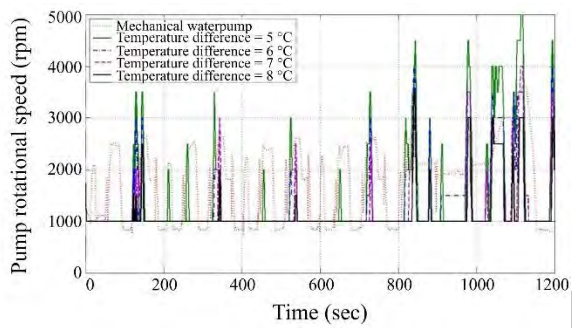

Figure 18. Comparison between mechanical water pump and electrical water pump operation for various inlet and outlet temperature differences and using an electrical fan and a heated thermostat

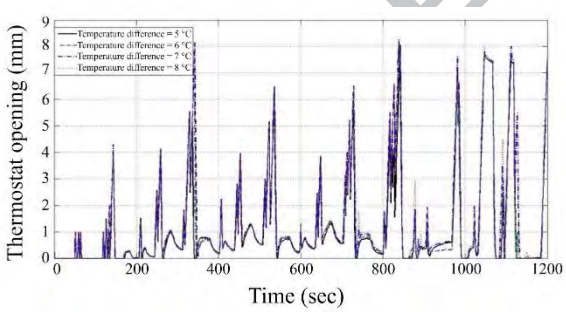

Figure 19. Comparison between heated thermostat operation for various engine inlet and outlet temperature differences with electrical water pump

Regardless of the inlet and outlet temperature difference, the electrical water pump reduces pump operation by over 50% compared to a mechanical water pump. For this reason, it is highly beneficial to substitute this controllable component for the conventional mechanical pump which, in addition to operating more continuously and requiring greater overall energy for operation, results in insufficient cooling performance in some situations.

For example, in comparison with the mechanical water pump, at a 7°C temperature difference between the inlet and outlet of engine, water pump energy is reduced 53.6% with an electrical water pump. For an 8°C difference, the total energy reduction is 60.8%. Note that in both of these cases, the reduced cooling due to the reduced activity of the electrical water pump is compensated by an increased opening of the heated thermostat. This can be seen in Fig. 18, which compares the heated thermostat operation for different temperature differences using an electrical water pump.

6. Conclusions

A controlling model for the cooling system of an engine was developed in order to reduce fuel consumption and engine emissions through the use of controllable engine cooling components including an electrical water pump, an electrical fan, and a heated thermostat. This model was based on engine characteristics that were derived from several experiments on a 1.4L engine. In this model, a control program is suggested that can control the different active intelligent components. The results of simulations using the derived engine model showed that fuel consumption decreases 1.1% for the intelligent cooling system under NEDC cycle operation compared to a conventional cooling system. Furthermore, using the intelligent cooling system results in a reduction in HC production of up to 5.3% and CO production of up to 6.1%.

Not all engine starts are cold starts, and it is common that an engine will be started again before the engine coolant has reached ambient temperature. In this case, the integration of an electrical water pump is greatly beneficial. For instance, if the initial coolant temperature is equal to 80°C, the energy consumption for an electrical water pump is less than half of that of a mechanical water pump.

Another potential advantage of replacing the mechanical water pump is that the hoses and connecting tubes and machinery can also be eliminated and/or repositioned potentially minimizing the size of the engine compartment. Moreover, in conventional systems the water pump is attached to the engine directly, placing restrictions on the water pump location which often result in a non-optimal design. Using an electrical water pump, one can optimize the utilization of engine compartment space and make it smaller.

Considering both the potential fuel savings and emission reductions, it is recommended to substitute the active controllable components described in this work for conventional mechanical components that provide insufficient cooling during various engine operation conditions while requiring greater energy to operate.

Acknowledgments

The authors gratefully acknowledge the Irankhodro Powertrain Company (IPCO) for supplying the required data for engine and cooperation in implement of experiments.

Nomenclature

c: tolerance

$\dot{m}$: mass flow rate, kg/min

Q: volume flow rate, m^3/min

q: Heat flux, Kw

RPM: motor rotational speed, rpm

T: temperature, °C

V: velocity

v: volume , m^3

X: thermostat opening level, mm

TWOT: engine outlet coolant temperature

Subscripts

amb: ambient

des: desired

eng: coolant flowing in engine property

max: maximum

min: minimum

mix: mixture

out_next_step: coolant leaving property at the next step

rad: coolant flow through radiator

sp: adjusted

veh: Vehicle

References

[1] R. Cipollone, D. Di Battista, G. Contaldi, S. Murgia, M. Mauriello, Development of a Sliding Vane Rotary Pump for Engine Cooling, Energy Procedia, 81 (2015) 775-783.

[2] P. Iodice, A. Senatore, G. Meccariello, M.V. Prati, Methodology for the analysis of a 4-stroke moped emission behaviour, SAE Int. J. Engines, 2 (2009) 617-626.

[3] R. Cipollone, D. Di Battista, Performances and Opportunities of an Engine Cooling System with a Double Circuit at Two Temperature Levels, in, SAE International, 2012.

[4] P. Lu, Q. Gao, Y. Wang, The simulation methods based on 1D/3D collaborative computing for the vehicle integrated thermal management, Applied Thermal Engineering, 104 (2016) 42-53.

[5] I.K. Yoo, K. Simpson, M. Bell, S. Majkowski, An engine coolant temperature model and application for cooling system diagnosis, SAE International, (2000).

[6] R.D.C. Jr., Thermal comfort and engine warm-up optimization of a low-flow advanced thermal management system, SAE International, (2004).

[7] N.-S. Ap, M. Tarquis, Innovative engine cooling systems comparison, SAE International, (2005).

[8] M. Chanfreau, B. Gessier, A. Farkh, P.Y. Geels, The need for an electrical water valve in a THErmal management intelligent system (THEMIS™), SAE International, (2003).

[9] F.W. Koch, F.G. Haubner, Cooling system development and optimization for DI engines, SAE International, (2000).

[10] J.R. Wagner, M.C. Ghone, D.W. Dawson, E.E. Marotta, Coolant flow control strategies for automotive thermal management systems, SAE International, (2002).

[11] J.R. Wagner, E.E. Marotta, I. Paradis, Thermal modeling of engine components for temperature prediction and fluid flow regulation, SAE International, (2001).

[12] G.M. Rocklage, G. Riehl, R. Vogt, Requirements on new components for future cooling systems, SAE International, (2001).

[13] T. Banjac, J.C. Wurzenberger, T. Katrašnik, Assessment of engine thermal management through advanced system engineering modeling, Advances in Engineering Software, 71 (2014) 19-33.

[14] P. Iodice, A. Senatore, Analysis of a Scooter Emission Behavior in Cold and Hot Conditions: Modelling and Experimental Investigations, in, SAE International, 2012.

[15] P. Iodice, A. Senatore, Engine and After-Treatment System Performance within the Cold Start Transient: New Modelling and Experiments, in, SAE International, 2015.

[16] P. Iodice, A. Senatore, Exhaust emissions of new high-performance motorcycles in hot and cold conditions, International Journal of Environmental Science and Technology, 12 (2015) 3133-3144.
[17] R. Burke, C. Brace, A. Cox, A. Lewis, J.G. Hawley, I. Pegg, R. Stark, Systems Approach to the Improvement of Engine Warm-Up Behaviour, Proceedings of the Institution of Mechanical Engineers, Part D: Journal of Automobile Engineering, 225 (2011) 190-205.
[18] R.D. Burke, C.J. Brace, J.G. Hawley, I. Pegg, Review of the systems analysis of interactions between the thermal, lubricant, and combustion processes of diesel engines, Proceedings of the Institution of Mechanical Engineers, Part D: Journal of Automobile Engineering, 224 (2010) 681-704.
[19] A. Lewis, C. Brace, S. Akehurst, K. Robinson, I. Pegg, Spatially resolved heat flux measurements from a HSDI engine over NEDC, in: Institution of Mechanical Engineers - VTMS 10, Vehicle Thermal Management Systems Conference and Exhibition, 2011, pp. 119-129.
[20] R.D. Burke, A.J. Lewis, S. Akehurst, C.J. Brace, I. Pegg, R. Stark, Systems optimisation of an active thermal management system during engine warm-up, Proceedings of the Institution of Mechanical Engineers, Part D: Journal of Automobile Engineering, 226 (2012) 1365-1379.
[21] B.K. Roy, N.K. Sharma, Control strategies for advanced thermal management system in IC engine, International Journal of Engineering Research and Technology, 6 (2013) 225-231.
[22] A. Lewis, C. Brace, S. Akehurst, K. Robinson, I. Pegg, Spatially resolved heat flux measurements from a HSDI engine over NEDC, in: Institution of Mechanical Engineers - VTMS 10, Vehicle Thermal Management Systems Conference and Exhibition, Woodhead Publishing Ltd., Cambridge, 2011, pp. 119-129.
[23] B. Zhou, X. Lan, X. Xu, X. Liang, Numerical model and control strategies for the advanced thermal management system of diesel engine, Applied Thermal Engineering, 82 (2015) 368-379.
[24] C.J. Brace, G. Hawley, S. Akehurst, M. Piddock, I. Pegg, Cooling system improvements - Assessing the effects on emissions and fuel economy, Proceedings of the Institution of Mechanical Engineers, Part D: Journal of Automobile Engineering, 222 (2008) 579-591.
[25] H. Cho, D. Jung, Z.S. Filipi, D.N. Assanis, J. Vanderslice, W. Bryzik, Application of controllable electric coolant pump for fuel economy and cooling performance improvement, Journal of Engineering for Gas Turbines and Power, 129 (2007) 239-244.
[26] Y.H. Shin, S.C. Kim, M.S. Kim, Use of electromagnetic clutch water pumps in vehicle engine cooling systems to reduce fuel consumption, Energy, 57 (2013) 624-631.
[27] E.S. Mohamed, Development and analysis of a variable position thermostat for smart cooling system of a light duty diesel vehicles and engine emissions assessment during NEDC, Applied Thermal Engineering, 99 (2016) 358-372.
[28] H. Kang, H. Ahn, K. Min, Smart cooling system of the double loop coolant structure with engine thermal management modeling, Applied Thermal Engineering, 79 (2015) 124-131.
[29] M.H. Salah, T.H. Mitchell, J.R. Wagner, D.M. Dawson, Nonlinear-control strategy for advanced vehicle thermal-management systems, IEEE Transactions on Vehicular Technology, 57 (2008) 127-137.
[30] P. Setlur, J.R. Wagner, D.M. Dawson, E. Marotta, An advanced engine thermal management system: Nonlinear control and test, IEEE/ASME Transactions on Mechatronics, 10 (2005) 210-220.
[31] N.-S. Ap, P. Guerrero, P. Jouanny, Influence of fan system electric power on the Heat performance of engine cooling module, SAE International, (2003).
[32] K.B. Kim, K.W. Choi, K.H. Lee, K.S. Lee, Active coolant control strategies in automotive engines, International Journal of Automotive Technology, 11 (2010) 767-772.
[33] E.D. Mohamed, Design and experimental investigation on an electromagnetic engine valve train, SAE Technical Papers, (2011).
[34] X. Wang, X. Liang, Z. Hao, R. Chen, Comparison of electrical and mechanical water pump performance in internal combustion engine, International Journal of Vehicle Systems Modelling and Testing, 10 (2015) 205-223.
[35] V. Negandhi, D. Jung, J. Shutty, Active thermal management with a dual mode coolant pump, SAE International, (2013).
[36] E. Cortona, C.H. Onder, Engine thermal management with electric cooling pump, SAE International, (2000).
[37] O. Armas, R. García-Contreras, Á. Ramos, Impact of alternative fuels on performance and pollutant emissions of a light duty engine tested under the new European driving cycle, Applied Energy, 107 (2013) 183-190.
[38] A. Choukroun, M. Chanfreau, Automatic control of electronic actuators for an optimized engine cooling thermal management, SAE International, (2001).
[39] J.R. Wagner, M.C. Ghone, D.W. Dawson, Coolant flow control strategies for automotive thermal management systems, SAE International, (2002).